RESEARCH ARTICLE

Thermal Conversion of Cobalt Based Hexacyanoferrates into Derived Cobalt Oxides for Supercapacitor Applications

Laiba Shah[1], Syeda Farahat Siddiqa[1], Javid Ullah[1], Atta Ullah[1], Adnan Sadiq[1], Ibrar Ahmad[1,2], Khizar Hayat[1,*] and Said Karim Shah[1,*]

[1] Department of Physics, Abdul Wali Khan University Mardan, Mardan 23200, Pakistan
[2] Department of Basic and Applied Sciences for Engineering, Sapienza University of Rome, Rome 00185, Italy

Abstract

We report the synthesis of cobalt-based hexacyanoferrate (Co-HCF) via a simple co-precipitation method and its subsequent conversion to a derived oxide through thermal treatment. Comprehensive characterization was performed using X-ray diffraction (XRD), Fourier transform infrared spectroscopy (FTIR), scanning electron microscopy (SEM), and energy-dispersive X-ray spectroscopy (EDX). XRD confirms the cubic crystal structure corresponding well to the JCPDS card no. 00-024-0327. FTIR confirms the presence of functional groups in Co-HCF, while the annealing process results in the complete removal of the cyanide ligands, yielding the derived oxide. SEM and EDX analyses confirm the cubic morphology and elemental composition of the prepared samples. Furthermore, electrochemical evaluation using cyclic voltammetry (CV) revealed that Co-HCF delivered a higher specific capacitance (C_s) of $624\,\mathrm{F\,g^{-1}}$ at $5\,\mathrm{mV\,s^{-1}}$, highlighting pseudocapacitive behavior due to its open framework structure and abundant redox-active cobalt centers. In contrast, the annealed sample exhibited comparatively lower C_s of $143\,\mathrm{F\,g^{-1}}$ under identical conditions, attributed to the partial collapse of the open HCF channels. This work demonstrates a controlled conversion route from Co-HCF to derived oxide, offering a promising pathway for next-generation supercapacitors (SCs) and sustainable energy storage technologies.

Keywords: cobalt hexacyanoferrates, thermal conversion, derived oxides, pseudocapacitor, cyclic voltammetry, kinetics.

1 Introduction

The world is facing an urgent energy crisis due to the rapid depletion of fossil fuels and the ever-growing global energy demand. Over-reliance on fossil fuels has led to serious consequences, such as increased

Submitted: 12 August 2025
Revised: 09 July 2026
Accepted: 18 July 2026
Published: 14 August 2026

Vol. 2, **No.** 3, 2026.
10.62762/JAEM.2026.780043

***Corresponding authors:**
✉ Khizar Hayat
khizarhayat@awkum.edu.pk
✉ Said Karim Shah
saidkarim@awkum.edu.pk

Citation
Shah, L., Siddiqa, S. F., Ullah, J., Ullah, A., Sadiq, A., Ahmad, I., Hayat, K., & Shah, S. K. (2026). Thermal Conversion of Cobalt Based Hexacyanoferrates into Derived Cobalt Oxides for Supercapacitor Applications. *Journal of Advanced Electronic Materials*, 2(3), 89–100.

carbon dioxide (CO_2) emissions and related hazards like climate change and global warming [1–4]. To overcome these challenges, it is essential to reduce reliance on fossil fuels and shift towards sustainable renewable energy sources such as solar, wind, and hydropower. However, the intermittent nature of these renewable energy sources necessitates the development of efficient energy storage and conversion technologies to provide a reliable power supply for electric vehicles, portable electronic devices, and grid-scale applications [5].

Supercapacitors are electrochemical energy storage devices that have attracted much attention due to their high-power density, fast charge and discharge capabilities, long cycle life, and excellent safety compared to traditional batteries such as fuel cells and lithium-ion batteries [6–14]. SCs fall between traditional capacitors and batteries, making them ideal for applications requiring high-power pulses. Based on their energy storage mechanism, SCs can be classified into three main categories: electric double-layer capacitors (EDLCs), pseudocapacitors, and hybrid supercapacitors. Pseudocapacitors utilize a rapid and reversible faradaic redox process to store energy near the surface of the electrode material [15, 16]. Electric double-layer capacitors (EDLCs) operate based on the separation of non-faradaic charges at the electrode-electrolyte interface. EDLCs offer high specific power density and cycle stability, but relatively low energy density. Pseudocapacitors, on the other hand, combine high energy density, moderate power output, and good cycle durability [17]. The hybrid supercapacitor combines the qualities of pseudocapacitor and EDLC and has better characteristics than individual components [18]. The electrochemical performance of supercapacitors mainly depends on the electrode materials that should possess high surface area, good electrical conductivity, abundant redox activity and structural stability [19–31].

Metal-organic frameworks (MOFs) have been designed as versatile precursors and templates for the derivation of high-performance electrode materials due to their crystalline porous structures with metal nodes connected by organic linkers [32, 33]. These materials possess very high surface areas, tunable pore sizes, flexible chemical compositions, and are thus ideal candidates for gas storage, separation, catalysis, and energy applications. MOFs can be directly used as electrodes or used as sacrificial precursors to synthesize metal oxides [34, 35], sulphides [27], phosphides or carbon composites [33, 36] with inherited hierarchical porosity and improved conductivity [36]. Their structural flexibility allows for precise engineering of the design of active sites and morphologies, overcoming limitations of traditional materials like agglomeration and poor ion diffusion [37, 38]. Recent advances have demonstrated that MOF-based electrodes can achieve superior specific capacitances, cycling stability and power densities in supercapacitors and batteries, making them the forerunners for next generation energy storage [39, 40].

A unique subclass of MOFs is hexacyanoferrate (HCF), with the general formula $A_xM[M'(CN)_6]_y{\cdot}nH_2O$, where A represents alkali metal cations and M, M′ denote the transition metals. PBAs have a highly open three-dimensional cubic framework with large interstitial channels, high specific surface area, tunable metal compositions and uniform distribution of redox-active sites [41, 42]. These structural features contribute to rapid ion diffusion and efficient mass transport. Furthermore, their low cost, room-temperature synthesis, and morphological diversity (cubes, hollow structures, or polyhedra) are beneficial for energy storage [41, 43]. Upon controlled thermal annealing, cyanide ligands decompose with gas evolution (e.g. CO_2, N_2) and lead to porous metal oxide derivatives with inherited precursor morphology [37, 44]. Cobalt-based hexacyanoferrate (Co-HCF) is especially promising due to the rich redox chemistry of its cobalt centers, fast faradaic charge and discharge, desirable ion mobility, and high porosity; its open framework structure enables rapid electrolyte ion intercalation/de-intercalation [45, 46]. The Co and Fe ions in Co-HCF undergo reversible redox reactions during the charge/discharge process, contributing to pseudocapacitive-like behavior, improved electron transfer, and enhanced overall performance, making them suitable for energy storage devices.

However, the thermal conversion at moderate temperature transforms the cyanide-bridged coordination polymer into spinel Co_3O_4 with optimized Co valence states, high surface area, and improved conductivity [44, 47, 48]. Recent studies on Co-HCF derived Co_3O_4 have reported that this precursor-derived approach often provides shorter diffusion paths, superior rate performance, better-exposed active sites, and good structural buffering during cycling, underscoring the effectiveness of this templating strategy [49, 50]. This thermal conversion involves a trade-off:

although annealing induces the collapse of the framework and formation of porous oxides with potentially improved stability and reduced framework degradation, it may also lead to a decrease in capacitance compared to Co-HCF due to partial loss of the highly open coordination framework structure and reduced accessibility of redox-active sites [49]. Yet, the derived oxides frequently exhibit superior long term stability and mechanical robustness, making them competitive for practical supercapacitor applications [51–53]. Metal-HCFs are promising candidates for electrochemical energy storage owing to their rich redox properties, which render them favorable electrode materials for pseudocapacitors [52].

In the present work, we study the transformation of as-synthesized Co-HCF to nanostructured derived oxide by a thermal treatment at 400 °C. This mild thermal treatment allows controlled framework collapse, complete removal of organic ligands and formation of derived oxide. A comprehensive comparative characterization of both the Co-HCF and derived oxide samples was performed by XRD to track phase transformation from cubic HCF to oxide, FTIR to monitor the disappearance of CN stretching vibrations and formation of Co-O bonds, SEM for surface and morphological evaluation, EDX to investigate the compositional changes with oxygen incorporation and CV for electrochemical evaluation, redox activity and pseudocapacitive performance [31]. The derived oxide sample shows a decrease in capacitance relative to Co-HCF, primarily due to structural densification, but exhibits enhanced cyclic stability [54, 55]. This study provides fundamental insights into the structure-property relationships during the PBA to oxide thermal conversion process, highlights a simple, sustainable route towards high-performance materials, which contributes to the ongoing development of HCF derived oxides as viable candidates for advanced sustainable energy technologies [48, 56–58].

2 Synthesis Procedures and Experimental Details

The synthesis method of Co-HCF was adopted from the reference [29], except by adding 0.2 mL of HCl rather than 0.1 mL into the solution. The obtained Co-HCF powder was annealed in air at 400 °C for 150 min to prepare its derived oxide. This moderate heat treatment condition was chosen to control the decomposition of cyanide ligands, framework collapse and conversion into derived oxide, while maintaining its overall morphology. The structure, morphology, composition and chemical properties of Co-HCF and its derived oxide were comprehensively analyzed by a variety of physical characterization techniques such as FTIR, XRD, SEM and EDX. XRD was used to study the phase purity and crystallinity of the sample using CuKα radiation ($\lambda = 1.5406$ Å). FTIR analysis was used to study the chemical bonds and functional groups in the sample. SEM and EDX were used to evaluate the morphology and elemental composition of the prepared sample. For electrochemical characterization, the electrode was prepared using the conventional method described in references [29, 59]. Briefly, the active material, carbon black, and polyvinylidene fluoride (PVDF) binder were mixed in a mass ratio of 80:10:10 in N-methyl-2-pyrrolidone (NMP) solvent. The resulting slurry was coated onto nickel foam current collectors with a typical active material mass loading of approximately 1–2 mg cm^{-2} and dried at 60 °C for 12 h before electrochemical testing. After preparation, the sample was characterized and finally tested as an electrode material for asymmetric supercapacitors on a potentiometer (Gamry Instruments 1000E). The working electrode in the three-electrode system is the Co-HCF or derived oxide sample, the reference electrode is Hg/Hg_2Cl_2, and the counter electrode is a platinum (Pt) wire.

3 Results and Discussion

3.1 Structural and Morphological Characterizations

The structural, elemental, chemical and morphological properties of Co-HCF and its derived oxide were comprehensively investigated using XRD, FTIR, SEM and EDX spectroscopy [53, 60]. The XRD pattern of Co-HCF, shown in Figure 1(a), displays sharp diffraction peaks that match well with the standard JCPDS card no. 00-024-0327. Prominent peaks appeared in the 2θ range of 15° to 60°. The calculated lattice parameter of 10.3 Å is in excellent agreement with the standard value of approximately 10.2–10.3 Å reported in the same card for $Co_3[Fe(CN)_6]_2{\cdot}nH_2O$. This close match confirms the successful formation of Co-HCF with high crystallinity, phase purity and structural integrity, consistent with the FCC cubic framework characteristic of metal hexacyanoferrate. The average crystallite size, calculated using the Williamson–Hall plot, was found to be 31.3 nm, and the microstrain was 5.7×10^{-4}. The open cubic structure with large interstitial channels is characteristic of HCF and efficient for ion diffusion in electrochemical

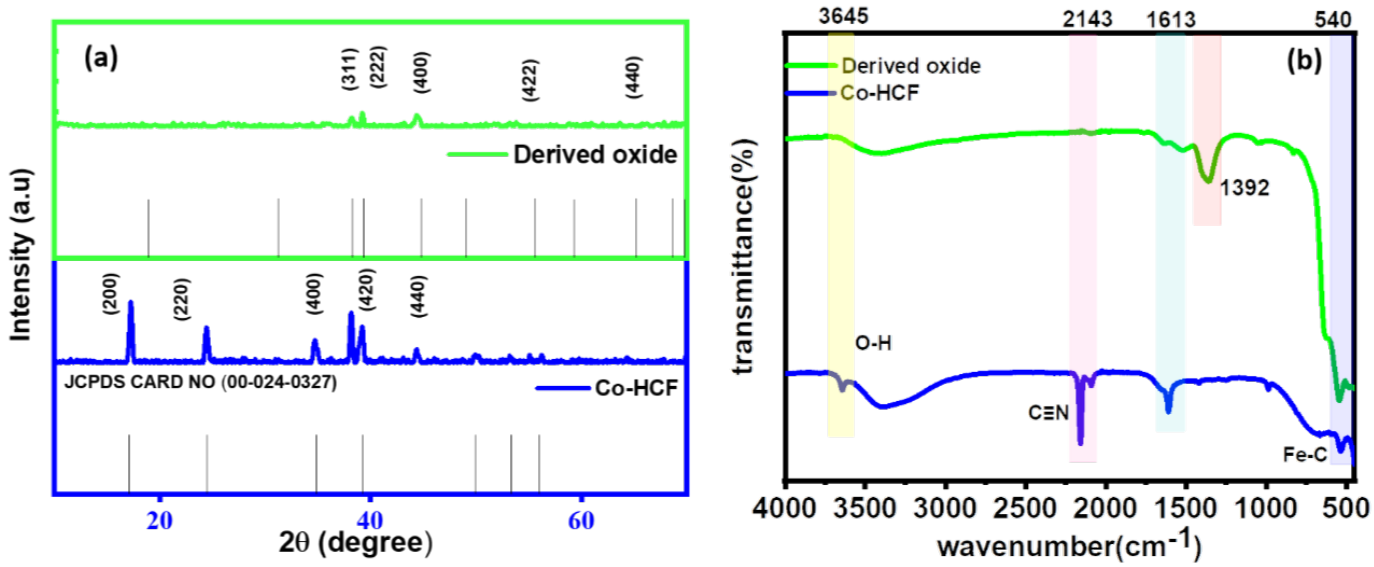

Figure 1. (a) XRD patterns, (b) FTIR spectra of Co-HCF and derived oxide.

applications [47, 49]. Nevertheless, in the XRD pattern of derived oxide, the characteristic HCF peaks disappear, and new diffraction peaks are observed in the 2θ range of 15° to 70°, indicating the spinel cubic phase of Co_3O_4. The peaks observed in the derived oxide do not follow the original HCF trend due to the collapse of the cyanide-bridged framework and formation of a dense spinel oxide structure. The crystallite size of derived Co_3O_4 slightly increases due to thermal treatment but remains in the nanoscale regime [29, 61, 62].

FTIR spectroscopy further confirmed the structural assessment of Co-HCF and derived oxide. The broad absorption peak observed around 3200–3644 cm^{-1} was associated with the O–H stretching vibrations, indicating the presence of adsorbed water and coordinated water molecules in the HCF framework [63]. The spectrum of Co-HCF, shown in Figure 1(b), displays a strong characteristic absorption band near 2090–2170 cm^{-1}, attributed to the C≡N stretching vibrations of the cyanide ligands (Co^{3+}–CN–Co^{2+} and related modes) [64, 65]. Other absorption bands near 1600–1650 cm^{-1} were associated with the bending vibrations of coordinated water and interstitial water molecules present in the HCF framework [59, 65]. The bending vibrations of metal-carbon (Fe-C) and cobalt-nitrogen (Co-N) bonds occur in the low frequency region at 600 and 505 cm^{-1} respectively [62, 64]. In derived oxide, the intense CN stretching bands completely disappear during annealing, confirming the successful removal of the cyanide groups through thermal decomposition. The bands emerging in the 550–670 cm^{-1} region are assigned to Co–O stretching vibrations of the Co_3O_4 lattice, confirming the conversion of the HCF framework into the derived oxide. The reduction of water-related bands indicates dehydration during thermal treatment [65].

SEM images reveal the morphological features of both samples, as shown in Figure 2(a, c). The Co-HCF exhibits well defined cubic morphology with relatively smooth surfaces, consistent with typical HCF morphologies obtained via co-precipitation [59]. After annealing the overall cubic morphology is mainly preserved, but the surface becomes rougher and more porous due to gas evolution during cyanide group decomposition. No severe agglomeration of the overall structure occurs at this optimized temperature [66, 67].

EDX analysis in Figure 2(b,d) confirms the elemental composition of the prepared samples. The Co-HCF spectrum shows the presence of cobalt (Co), carbon (C), oxygen (O), nitrogen (N) and minor potassium (K) from the precursor, with relatively the same expected ratios supporting the HCF framework. In the annealed sample, the carbon and nitrogen peaks significantly decrease, while the oxygen peak increases substantially [68], consistent with the formation of the derived oxide [62].

3.2 Electrochemical Performance

The electrochemical performance of as-synthesized Co-HCF and derived oxide was thoroughly evaluated using CV in a three-electrode configuration with 3 M KOH electrolyte. The Co-HCF and derived oxide were pasted on nickel foam and tested under identical

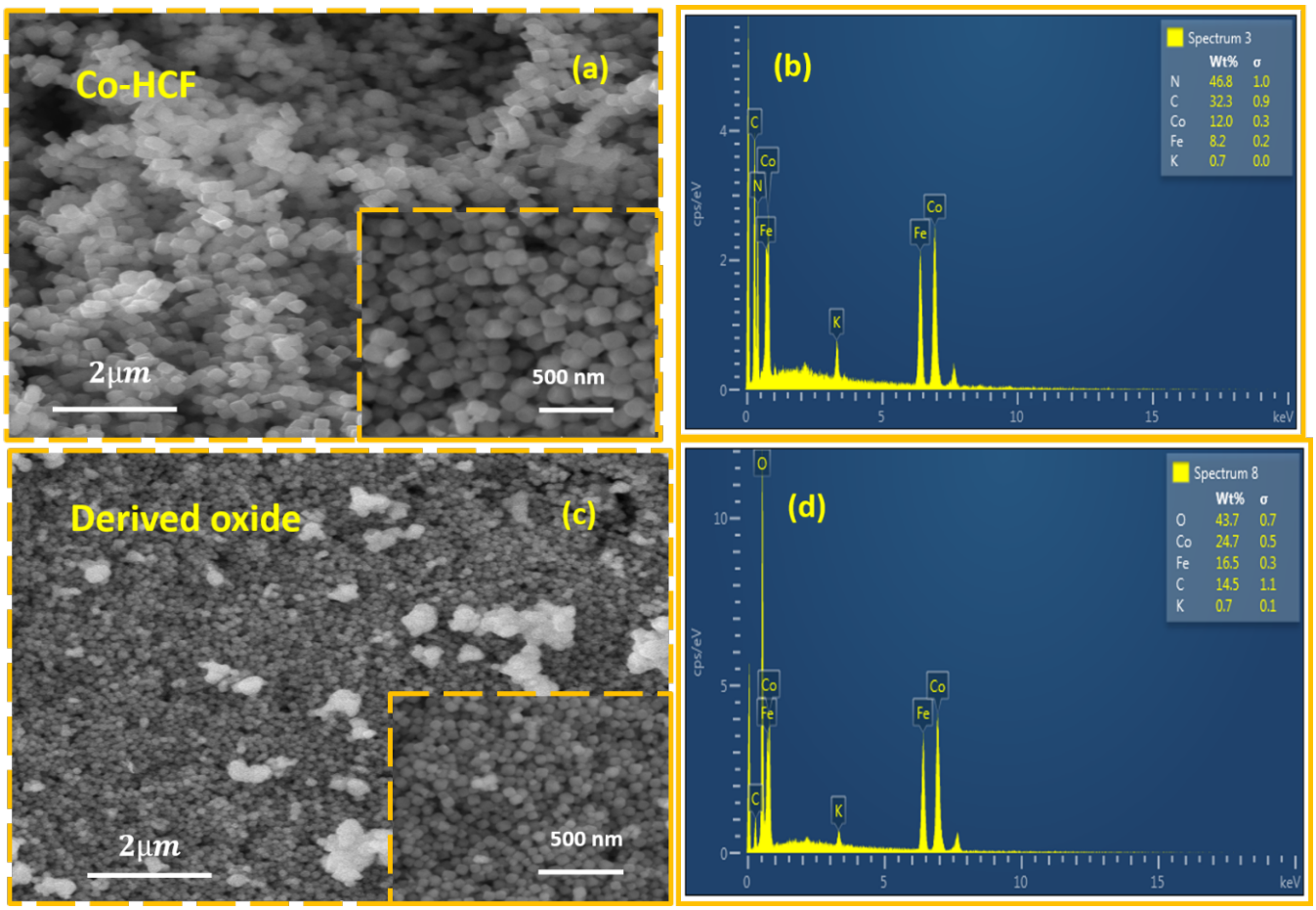

Figure 2. (a, c) FESEM images, (b, d) EDX spectra of Co-HCF and derived oxide.

conditions to enable direct comparison of the effect of thermal conversion on pseudocapacitive behavior.

Typically, CV curves of Co-HCF (Figure 3(a)) exhibit a pair of well-defined redox peaks within a potential window of 0.6 to 1.0 V, characteristic of Faradaic redox reactions associated with the reversible conversion between Co^{2+}/Co^{3+} oxidation states in the open HCF framework. CV measurements were performed at scan rates ranging from 5 to 100 mV s^{-1}, and the well-retained redox peak shapes indicate good rate capability and fast ion diffusion through the large interstitial channels of the cubic HCF structure. The specific capacitance calculated from CV curves, shown in Figure 3(b), reached a maximum value of $624\,F\,g^{-1}$ at $5\,mV\,s^{-1}$ for Co-HCF, demonstrating excellent pseudocapacitive performance. In contrast, as shown in Figure 3(c), the derived oxide shows redox peaks corresponding to the Co_3O_4 spinel phase but with slightly shifted peak positions and reduced peak currents [62]. The specific capacitance of the derived oxide, as shown in Figure 3(d), decreased to $143\,F\,g^{-1}$ at the same scan rate. This reduction is attributed to the partial collapse of the highly open cyanide-linked framework during thermal treatment, decreasing the number of readily accessible redox-active sites and ion intercalation channels despite the formation of a porous structure. Nevertheless, the CV curves of derived oxide maintain better symmetry and less distortion at high scan rates, which suggests improved reversibility [60, 69].

To better understand the charge storage mechanism, the CV curves were further investigated by the Randles–Ševčík and Dunn methods to study the charge storage behavior and reaction kinetics of both samples. The value of b provides insights into the nature of the charge storage process and was analyzed using the power law relationship $I_{pc} = av^b$, where I_{pc} is the peak current and v is the scan rate: a b value closer to 0.5 indicates a diffusion-controlled process, while a value near 1 signifies surface-controlled capacitive behavior [70, 71]. Figure 4(a) shows the fitting of the logarithm of peak currents (I_{pc}) versus the logarithm of scan rate (v) to obtain the b-values. The fitted b-values for Co-HCF and the derived oxide were determined to be 0.99 and 0.97, respectively. This demonstrates that the electrochemical response

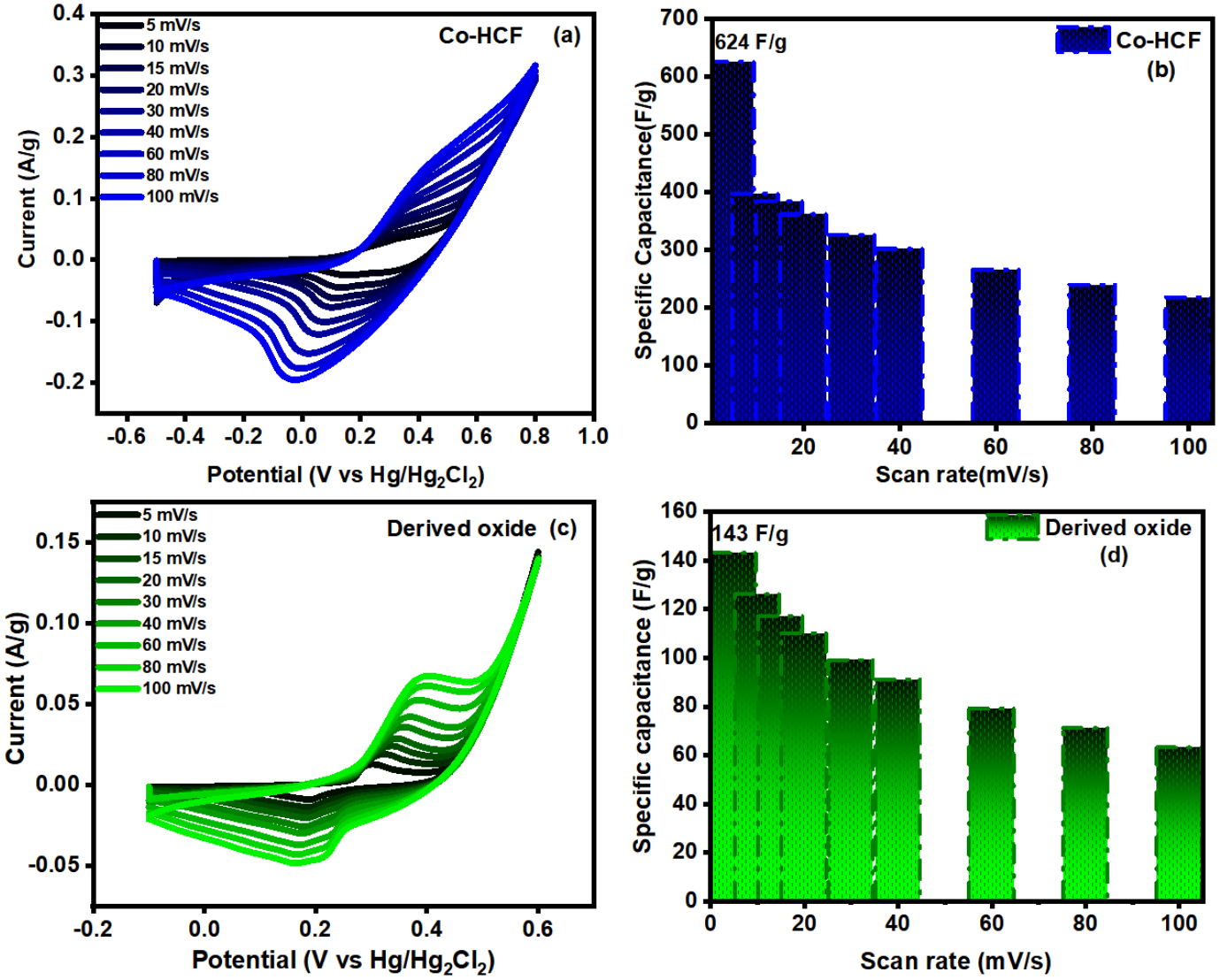

Figure 3. (a, c) CV curves at various scan rates, (b, d) C_s vs. ν plots of Co-HCF and derived oxide.

in both samples is dominated by surface-controlled pseudocapacitive process, which is highly desirable for supercapacitor applications as it enables fast charge/discharge and high rate capability. The slightly higher b value for Co-HCF underscores its more ideal capacitive characteristics, consistent with its higher specific capacitance, while the derived oxide still exhibits pseudocapacitive behavior with improved cyclic stability. This power-law kinetic analysis has been widely employed to distinguish capacitive from diffusion-controlled processes in pseudocapacitive electrode systems [70, 72]. Figure 4(b) plots the peak current/square root of scan rate ($I_p/v^{1/2}$) vs. the square root of scan rate ($v^{1/2}$), showing a strong linear relationship with a relatively good fitting parameter. Furthermore, the diffusive and capacitive contributions were calculated using Dunn's method as shown in Figure 4(c). It reveals that Co-HCF exhibits a dominant diffusion-controlled contribution (98%) at 20 mV/s, indicating that intercalation-type faradaic processes play a major role in charge storage through the open channels of the HCF framework. The annealed sample (Figure 4(d)) shows a slightly reduced diffusion-controlled contribution (91%) at the same scan rate, suggesting a modest increase in the surface capacitive fraction following thermal conversion. Taken together, the high b-values (0.99 and 0.97) and the dominant diffusion-controlled contributions indicate that the charge storage in both samples is governed by intercalation-type pseudocapacitive processes, which are fast and reversible due to the open framework and abundant redox-active cobalt centers [60, 70].

4 Conclusions

In summary, the Co-HCF was successfully synthesized via a simple and cost-effective co-precipitation method.

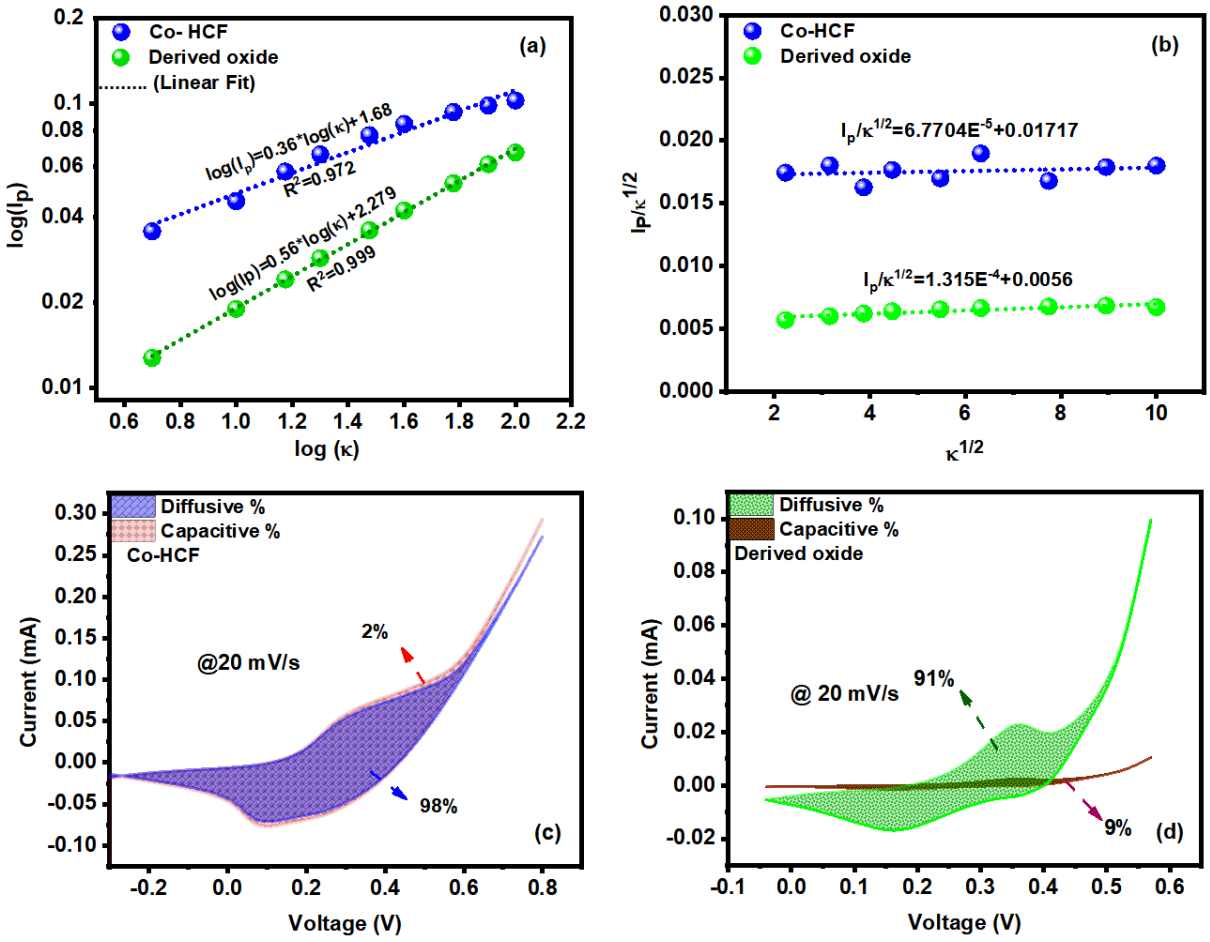

Figure 4. (a) slope of log I_{pc} vs. v to calculate 'b' values, (b) slope line between $I_{pc}/v^{1/2}$ vs. $v^{1/2}$, (c, d) capacitive and diffusive contribution at 20 mV/s of Co-HCF and derived oxide.

The prepared Co-HCF was annealed in air at 400 °C for 150 min to further transform it into a derived oxide. Physicochemical characterization using XRD, FTIR, SEM, and EDX confirmed the complete transformation of the Co-HCF framework into derived oxide. The annealing process thoroughly removed the cyanide ligands, resulting in favorable porosity while maintaining the overall cubic morphology and increasing surface roughness. Electrochemical studies in KOH electrolyte showed that the synthesized Co-HCF electrode exhibited excellent pseudocapacitive performance. Its open three-dimensional framework and abundant redox-active cobalt sites promoted rapid ion diffusion and Faradaic reactions, achieving an excellent specific capacitance of $624\,\mathrm{F\,g^{-1}}$ at a scan rate of $5\,\mathrm{mV\,s^{-1}}$. The derived oxide electrode after thermal conversion exhibited a lower specific capacitance of approximately $143\,\mathrm{F\,g^{-1}}$ under the same conditions. The reduction is primarily attributable to the partial collapse of the highly open HCF structure and lower accessibility of the redox sites. However, the derived oxide showed significantly enhanced cycling stability and improved electrochemical reversibility than the Co-HCF owing to the robust Co_3O_4 phase and improved structural integrity. The present study highlights the trade-off between high initial capacitance of the precursor Co-HCF and the excellent long-term stability of derived oxide. This controllable thermal conversion strategy provides a facile and scalable approach to design stable earth-abundant pseudocapacitive materials for supercapacitor applications. The results provide fundamental insights into the structure-property relationships during the HCF to metal oxide transformation and show the potential of HCF-derived oxides as promising electrode materials for the next generation of sustainable energy storage devices. Further optimization of the annealing conditions or incorporation of conductive additives and composite architectures represents a promising avenue for future work aimed at enhancing the capacitance of the derived oxide while retaining its excellent long-term stability.

Data Availability Statement

Data will be made available on request.

Funding

This work was supported by the Higher Education Commission (HEC), Islamabad, Pakistan, under Grant 20-140245-75/NRPU/R&ID/HEC/2026.

Conflicts of Interest

The authors declare no conflicts of interest.

AI Use Statement

The authors declare that no generative AI was used in the preparation of this manuscript.

Ethical Approval and Consent to Participate

Not applicable.

References

[1] Kumar, N., Kim, S. B., Lee, S. Y., & Park, S. J. (2022). Recent advanced supercapacitor: a review of storage mechanisms, electrode materials, modification, and perspectives. *Nanomaterials, 12*(20), 3708. [CrossRef]

[2] Lim, J. M., Jang, Y. S., Van T. Nguyen, H., Kim, J. S., Yoon, Y., Park, B. J., ... & Doo, S. G. (2023). Advances in high-voltage supercapacitors for energy storage systems: materials and electrolyte tailoring to implementation. *Nanoscale Advances, 5*(3), 615-626. [CrossRef]

[3] Lakshmi, K. S., & Vedhanarayanan, B. (2023). High-performance supercapacitors: a comprehensive review on paradigm shift of conventional energy storage devices. *Batteries, 9*(4), 202. [CrossRef]

[4] Koohi-Fayegh, S., & Rosen, M. A. (2020). A review of energy storage types, applications and recent developments. *Journal of energy storage, 27*, 101047. [CrossRef]

[5] Thuy, V. V., Hieu, N. S., & Thu, T. V. (2024). Novel mixed nickel/cobalt hexacyanoferrate microcubes with synergistic effects for aqueous hybrid supercapacitors. *Dalton Transactions, 53*(42), 17333-17342. [CrossRef]

[6] Du, X., Ren, H., Liang, J., & Wu, W. (2025). Prussian blue and its analogues for flexible electrochemical energy storage: from materials to devices. *Applied Physics Reviews, 12*(2). [CrossRef]

[7] Choi, C., Ashby, D. S., Butts, D. M., DeBlock, R. H., Wei, Q., Lau, J., & Dunn, B. (2020). Achieving high energy density and high power density with pseudocapacitive materials. *Nature Reviews Materials, 5*(1), 5-19. [CrossRef]

[8] Zhu, X., Tao, H., & Li, M. (2020). Co-precipitation synthesis of nickel cobalt hexacyanoferrate for binder-free high-performance supercapacitor electrodes. *International Journal of Hydrogen Energy, 45*(28), 14452-14460. [CrossRef]

[9] Kim, J., Yi, S. H., Li, L., Thu, T. V., & Chun, S. E. (2022). Effect of valence state of cobalt in cobalt hexacyanoferrate coprecipitated at different temperatures on electrochemical behavior. *International Journal of Energy Research, 46*(15), 22717-22729. [CrossRef]

[10] Samyn, L. M., Lessa, T. S., Babu, R. S., Kalaivani, A., Barbosa, T. M., & De Barros, A. L. F. (2023). High-performance flexible supercapacitors based on potassium nickel (ii) hexacyanoferrates (iii) nanoparticles on carbon cloth as an electrode material. *Materials Advances, 4*(16), 3654-3661. [CrossRef]

[11] Shao, Y., El-Kady, M. F., Sun, J., Li, Y., Zhang, Q., Zhu, M., ... & Kaner, R. B. (2018). Design and mechanisms of asymmetric supercapacitors. *Chemical reviews, 118*(18), 9233-9280. [CrossRef]

[12] González, A., Goikolea, E., Barrena, J. A., & Mysyk, R. (2016). Review on supercapacitors: Technologies and materials. *Renewable and sustainable energy reviews, 58*, 1189-1206. [CrossRef]

[13] Conway, B. E., Birss, V., & Wojtowicz, J. (1997). The role and utilization of pseudocapacitance for energy storage by supercapacitors. *Journal of power sources, 66*(1-2), 1-14. [CrossRef]

[14] Khan, K., Shah, M. Z. U., Aziz, U., Hayat, K., Sajjad, M., Ahmad, I., ... & Shah, A. (2022). Development of 1.6 V hybrid supercapacitor based on ZnO nanorods/MnO2 nanowires for next-generation electrochemical energy storage. *Journal of Electroanalytical Chemistry, 922*, 116753. [CrossRef]

[15] Chen, R., Yu, M., Sahu, R. P., Puri, I. K., & Zhitomirsky, I. (2020). The development of pseudocapacitor electrodes and devices with high active mass loading. *Advanced Energy Materials, 10*(20), 1903848. [CrossRef]

[16] Costentin, C., & Savéant, J. M. (2019). Energy storage: pseudocapacitance in prospect. *Chemical Science, 10*(22), 5656-5666. [CrossRef]

[17] Liang, R., Du, Y., Xiao, P., Cheng, J., Yuan, S., Chen, Y., ... & Chen, J. (2021). Transition metal oxide electrode materials for supercapacitors: a review of recent developments. *Nanomaterials, 11*(5), 1248. [CrossRef]

[18] An, C., Wang, Y., Jiao, L., & Yuan, H. (2016). Mesoporous Ni@ C hybrids for a high energy aqueous asymmetric supercapacitor device. *Journal of Materials Chemistry A, 4*(24), 9670-9676. [CrossRef]

[19] Rauf, M., Shah, S. S., Shah, S. K., Shah, S. N. A., Haq, T. U., Shah, J., ... & Hayat, K. (2022). Facile hydrothermal synthesis of zinc sulfide nanowires for high-performance asymmetric supercapacitor. *Journal of Saudi Chemical Society, 26*(4), 1-13. [CrossRef]

[20] Nasrullah, Wisal, W., Bibi, F., Shah, S. K., Ullah,

J., Rauf, M., ... & Hayat, K. (2026). Electrospun SnO2/Co3O4 Core–Shell Nanofibers Decorated with ZnO for High Performance Asymmetric Supercapacitors. *Journal of Inorganic and Organometallic Polymers and Materials*, 1-17. [CrossRef]

[21] Bibi, F., Ahmad, I., Shah, S. S., Shah, J., Samreen, A., Shah, S. K., ... & Hayat, K. (2025). Facile and sustainable fabrication of TiO2/Co3O4 core-shell fiber electrodes for enhanced electrochemical performance in asymmetric supercapacitors. *Materials Research Bulletin*, 113843. [CrossRef]

[22] Rehman, Z. U., Ullah, J., Anum, K., Hayat, K., Shah, S. K., & Gunnella, R. (2026). Viability of Co_3O_4/TiO_2 Composite as Electrode Materials for Supercapacitor and efficient OER/HER Electrocatalysis. *Materials Research Bulletin*, 114204. [CrossRef]

[23] Jiang, H., Chen, J., Shi, Y., Chen, P., Tang, X., Jiang, W., ... & Wu, G. (2022). A wearable all-solid-state supercapacitor with extremely high stability based on 2D Co-HCF/GO. *Applied Surface Science, 586*, 152739. [CrossRef]

[24] Al Kiey, S. A., & Abdelhamid, H. N. (2022). Metal-organic frameworks (MOFs)-derived Co3O4@ N-doped carbon as an electrode materials for supercapacitor. *Journal of Energy Storage, 55*, 105449. [CrossRef]

[25] Shah, M. Z. U., Shah, J., Hayat, K., Shah, S. K., Hussain, I., Khan, A. U., ... & Shah, A. (2024). Optimizing performance: achieving high capacitance and cycling durability in alkaline electrolyte with SnO2/SnSe‖ AC/KOH-based aqueous hybrid supercapacitor. *Journal of Energy Storage, 75*, 109662. [CrossRef]

[26] Kumar, R., Soam, A., & Sahajwalla, V. (2021). Carbon coated cobalt oxide (CC-CO3O4) as electrode material for supercapacitor applications. *Materials Advances, 2*(9), 2918-2923. [CrossRef]

[27] Zeng, X., Yang, B., Li, X., & Yu, R. (2017). Three-dimensional hollow CoS2 nanoframes fabricated by anion replacement and their enhanced pseudocapacitive performances. *Electrochimica Acta, 240*, 341-349. [CrossRef]

[28] Villalva-Mejorada, D. I., Acevedo-Peña, P., Leyva-Porras, C., Rodríguez-Hernández, J., & Reguera, E. (2022). Mixed cobalt–zinc hexacyanoferrate hollow micro–cubes for a high–voltage hybrid supercapacitor. *International Journal of Energy Research, 46*(15), 23310-23325. [CrossRef]

[29] Sadiq, A., Shah, S. K., Ullah, A., Ahmad, I., Ullah, J., Usman, M., ... & Gunnella, R. (2026). Exploring cobalt-based Prussian blue analogue for sustainable energy storage and biomedical applications. *Electrochimica Acta*, 148725. [CrossRef]

[30] Gaikwad, P., Tiwari, N., Kamat, R., Mane, S. M., & Kulkarni, S. B. (2024). A comprehensive review on the progress of transition metal oxides materials as a supercapacitor electrode. *Materials Science and Engineering: B, 307*, 117544. [CrossRef]

[31] Cui, D., Wang, R., Qian, C., Shen, H., Xia, J., Sun, K., ... & Bao, W. (2023). Achieving high performance electrode for energy storage with advanced prussian blue-drived nanocomposites—a review. *Materials, 16*(4), 1430. [CrossRef]

[32] Baumann, A. E., Burns, D. A., Liu, B., & Thoi, V. S. (2019). Metal-organic framework functionalization and design strategies for advanced electrochemical energy storage devices. *Communications Chemistry, 2*(1), 86. [CrossRef]

[33] Bhoite, A. A., Patil, K. V., Redekar, R. S., Jang, J. H., Sawant, V. A., & Tarwal, N. L. (2023). Recent advances in Metal-Organic Framework (MOF) derived metal oxides and their composites with carbon for energy storage applications. *Journal of Energy Storage, 72*, 108557. [CrossRef]

[34] Zhou, L., Li, C., Liu, X., Zhu, Y., Wu, Y., & Van Ree, T. (2018). Metal oxides in supercapacitors. In *Metal oxides in energy technologies* (pp. 169-203). Elsevier. [CrossRef]

[35] Moradi, M., Afkhami, A., Madrakian, T., & Moazami, H. R. (2022). Hydrothermal synthesis of nanocages of Mn-Co Prussian blue analogue and charge storage investigation of the derived Mn-Co oxide@/rGO composites. *FlatChem, 32*, 100350. [CrossRef]

[36] Du, W., Bai, Y. L., Xu, J., Zhao, H., Zhang, L., Li, X., & Zhang, J. (2018). Advanced metal-organic frameworks (MOFs) and their derived electrode materials for supercapacitors. *Journal of Power Sources, 402*, 281-295. [CrossRef]

[37] Goda, E. S., Lee, S., Sohail, M., & Yoon, K. R. (2020). Prussian blue and its analogues as advanced supercapacitor electrodes. *Journal of Energy Chemistry, 50*, 206-229. [CrossRef]

[38] Nai, J., & Lou, X. W. (2019). Hollow structures based on prussian blue and its analogs for electrochemical energy storage and conversion. *Advanced Materials, 31*(38), 1706825. [CrossRef]

[39] Xiong, C., Zhang, Y., Zheng, C., Yin, Y., Xiong, Q., Zhao, M., & Wang, B. (2024). Fabrication of metal-organic framework@ cellulose nanofibers/reduced graphene oxide-Vitrimer composite electrode materials with shape memory for supercapacitors. *Electrochimica Acta, 493*, 144373. [CrossRef]

[40] Zhang, Y., Xiong, C., Xiong, Q., Xiong, Q., Zhao, M., Wang, B., ... & Ni, Y. (2025). Ni, Co bimetallic MOF of dual-controlled by micro-morphology and unit cell structure for biomass-based self-supporting energy storage device. *Rare Metals, 44*(11), 8536-8547. [CrossRef]

[41] Kitchamsetti, N. (2023). A review on recent advances in Prussian blue, its analogues, and their derived materials as electrodes for high performance supercapacitors. *Journal of Energy Storage, 73*, 108958.

[CrossRef]

[42] Wei, Y., Zheng, M., Zhu, W., & Pang, H. (2023). Hollow structures Prussian blue, its analogs, and their derivatives: Synthesis and electrochemical energy-related applications. *Carbon Neutralization, 2*(3), 271-299. [CrossRef]

[43] Liang, J., Tian, B., Zhang, X., Jiang, C., He, D., & Wu, W. (2023). Surface-defect engineering of a nickel hexacyanoferrate material for high-performance printed flexible supercapacitors. *Journal of Materials Chemistry A, 11*(7), 3493-3503. [CrossRef]

[44] Lin, Y., Zhang, L., Xiong, Y., Wei, T., & Fan, Z. (2020). Toward the design of high-performance supercapacitors by prussian blue, its analogues and their derivatives. *Energy & Environmental Materials, 3*(3), 323-345. [CrossRef]

[45] Fu, X., Ren, L., Tian, H., Sun, Z., Jin, Y., Wang, D., ... & Yang, H. (2024). Facile synthesis of cryogenically controlled cobalt-nickel-based Prussian blue analogues for high-performance symmetric supercapacitors. *Journal of Alloys and Compounds, 992*, 174606. [CrossRef]

[46] Arunkumar, K., Kamalakkannan, D., Kamalarajan, P., Chanthirasekaran, K., Kumaran, S., & Basha, C. Z. (2026). Boosting the electrochemical performance of cobalt hexacyanoferrate via sulfur-doped reduced graphene oxide hybridization. *Ionics, 32*(3), 3593-3609. [CrossRef]

[47] Kanimozhi, S. N., Roy, S., Alswieleh, A. M., Subbiah, J., & Sambandam, A. (2024). Zinc tailored cobalt Prussian blue analogue (PBA) as a prospective candidate for supercapacitor applications. *ACS Applied Electronic Materials, 6*(11), 7799-7808. [CrossRef]

[48] Lu, C., Yang, Y., Li, S., & Zhu, M. (2024). Nanosheet floral clusters of Fe-doped Co3O4 for high-performance supercapacitors. *Materials Chemistry Frontiers, 8*(10), 2282-2292. [CrossRef]

[49] Ju, H., Yang, J., Guo, X., Lang, H., Wang, S., Pu, C., ... & Han, W. (2024). Prussian blue analogue-derived Co3O4/Fe2O3 with a partially hollow and octahedral structure for high-performance supercapacitors. *Dalton Transactions, 53*(6), 2626-2634. [CrossRef]

[50] Song, X., Song, S., Wang, D., & Zhang, H. (2021). Prussian blue analogs and their derived nanomaterials for electrochemical energy storage and electrocatalysis. *Small Methods, 5*(4), 2001000. [CrossRef]

[51] Hurlbutt, K., Wheeler, S., Capone, I., & Pasta, M. (2018). Prussian blue analogs as battery materials. *Joule, 2*(10), 1950-1960. [CrossRef]

[52] Ju, H., Liu, X. D., Tao, C. Y., Yang, F., Liu, X. L., Luo, X., & Zhang, L. (2021). Prussian blue analogue derived low-crystalline Mn2O3/Co3O4 as high-performance supercapacitor electrode. *Journal of Alloys and Compounds, 856*, 157134. [CrossRef]

[53] Hu, B., Jiang, J., Wang, P., Cheng, H., Li, D., Zhou, Z., ... & Li, Z. (2025). Prussian-blue-analogue-derived Ag@ Co3O4 and Bi2O3@ BiFeO3 nanostructures as battery-type electrodes for high-performance asymmetric supercapacitor. *ACS Applied Nano Materials, 8*(1), 720-732. [CrossRef]

[54] Mohammadi, S., Targholi, E., & Mousavi-Khoshdel, S. M. (2021). Metal–organic framework-derived cobalt hydroxide microparticles as supercapacitor electrode materials. *Journal of the Iranian Chemical Society, 18*(8), 2115-2122. [CrossRef]

[55] Bao, Y., Chen, G., Zhu, X., Zou, P., Yang, Q., Yuan, S., & Chen, C. (2025). Encapsulation of cobalt-iron Prussian blue analog nanocubes using a redox polymer for advanced supercapacitor cathode materials. *Journal of Colloid and Interface Science, 697*, 137975. [CrossRef]

[56] Fayaz, M., Lai, W., Li, J., Chen, W., Luo, X., Wang, Z., ... & Chen, Y. (2024). Prussian blue analogues and their derived materials for electrochemical energy storage: Promises and Challenges. *Materials Research Bulletin, 170*, 112593. [CrossRef]

[57] Garcia, M. F., Arzuza, L. C., Neves, G. A., Loureiro, F. J., Morales, M. A., Macedo, D. A., ... & Menezes, R. R. (2025). Structure and morphological properties of cobalt-oxide-based (Co3O4) materials as electrodes for supercapacitors: a brief review. *Materials, 18*(2), 413. [CrossRef]

[58] Janani, G., Park, S., Surendran, S., Lim, Y., Moon, D. J., Jeong, G. H., ... & Sim, U. (2025). Strategic insights into Prussian Blue Analogues-based catalysts: Design and regulation for enhanced electrochemical energy storage and conversion. *Next Materials, 9*, 100930. [CrossRef]

[59] Ullah, A., Sadiq, A., Usman, M., Ahmad, I., Sher, A., Rehman, G., ... & Gunnella, R. (2025). Facile synthesis of zinc-based Prussian blue analogue (Zn-PBAs) for supercapacitor and biomedical applications. *Sustainable Materials and Technologies, 44*, e01357. [CrossRef]

[60] Abdullin, K. A., Gabdullin, M. T., Kalkozova, Z. K., Nurbolat, S. T., & Mirzaeian, M. (2022). Efficient recovery annealing of the pseudocapacitive electrode with a high loading of cobalt oxide nanoparticles for hybrid supercapacitor applications. *Nanomaterials, 12*(20), 3669. [CrossRef]

[61] Ashfaq, H. T., Asghar, M. A., Nisar, T., Wagner, V., Mansoor, M. A., Haider, A., & Ali, S. (2023). Electrochemical synthesis of Co-, Ni-and NiCo-based hexacyanocobaltates as efficient electrocatalysts for water oxidation studies. *Inorganic Chemistry Communications, 154*, 110916. [CrossRef]

[62] Agilandeswari, K., & Rubankumar, A. (2016). Synthesis, characterization, optical, and magnetic properties of Co3O4 nanoparticles by quick precipitation. *Synthesis and Reactivity in Inorganic, Metal-Organic, and Nano-Metal Chemistry, 46*(4), 502-506. [CrossRef]

[63] Zhu, P., Li, X., Yao, H., & Pang, H. (2020). Hollow cobalt-iron prussian blue analogue nanocubes for high-performance supercapacitors. *Journal of Energy Storage, 31*, 101544. [CrossRef]

[64] Liu, Y., Hu, X., He, H., Li, J., Dong, H., Shearing, P. R., ... & Brett, D. J. (2023). Polyaniline–Cobalt Hexacyanoferrate Composites as High-Performance Cathodes for Zn-Ion Hybrid Supercapacitor. *Energy Technology, 11*(11), 2201368. [CrossRef]

[65] Pires, B. M., Nunes, W. G., Freitas, B. G., Oliveira, F. E. R., Katic, V., Rodella, C. B., ... & Zanin, H. (2021). Characterization of porous cobalt hexacyanoferrate and activated carbon electrodes under dynamic polarization conditions in a sodium-ion pseudocapacitor. *Journal of energy chemistry, 54*, 53-62. [CrossRef]

[66] Carvalho, C. L., Silva, A. T., Macedo, L. J., Luz, R. A., Neto, J. M. M., & Cantanhêde, W. (2015). New hybrid nanomaterial based on self-assembly of cyclodextrins and cobalt prussian blue analogue nanocubes. *International Journal of Molecular Sciences, 16*(7), 14594-14607. [CrossRef]

[67] Zhao, C., Chen, Q., Jiang, L., Liu, Z., Liao, X., Qi, Y., & Chen, W. (2025). Hierarchical porous co-Mn Hexacyanoferrate for advanced aqueous sodium-ion hybrid supercapacitors. *Journal of The Electrochemical Society, 172*(1), 010517. [CrossRef]

[68] Siddiqa, S. F., Ullah, A., Shah, S. K., Ullah, J., Ahmad, I., Rauf, M., ... & Gunnella, R. (2026). Structural engineering of Cobalt Prussian blue analogues for enhanced electrochemical and electrocatalytic performance. *Journal of Energy Storage, 177*, 123486. [CrossRef]

[69] Zhao, F., Wang, Y., Xu, X., Liu, Y., Song, R., Lu, G., & Li, Y. (2014). Cobalt hexacyanoferrate nanoparticles as a high-rate and ultra-stable supercapacitor electrode material. *ACS applied materials & interfaces, 6*(14), 11007-11012. [CrossRef]

[70] Pervez, S., & Iqbal, M. Z. (2023). Capacitive and Diffusive Contributions in Supercapacitors and Batteries: A Critique of b-Value and the v–v1/2 Model. *Small, 19*(48), 2305059. [CrossRef]

[71] Lether, F. G., & Wenston, P. R. (1987). An algorithm for the numerical evaluation of the reversible Randles-Sevcik function. *Computers & chemistry, 11*(3), 179-183. [CrossRef]

[72] Rafique, A., Naeem, U., Marques, A., Ferreira, I., Rizwan, S., & Baptista, A. C. (2025). Understanding the capacitive and diffusion-controlled behavior of electrophoretically deposited V2CTx on carbon yarn as a potential anode for asymmetric devices. *ACS omega, 10*(8), 7621. [CrossRef]

Laiba Shah received her MPhil in Physics from Abdul Wali Khan University Mardan, Khyber Pakhtunkhwa, Pakistan, in 2025. Her research focused on Material Science, particularly the development of materials for storage devices. (Email: syednizakatullahs@gmail.com)

Syeda Farahat Siddiqa is currently pursuing her PhD in Physics from Abdul Wali Khan University Mardan (AWKUM) and completed her MPhil in Physics in 2024 from the same University. Her research was focused on Materials Science, with particular emphasis on the design, synthesis, and characterization of advanced materials for energy storage devices. (Email: syedasiddiqa522@gmail.com)

Javid Ullah has completed his BS in Physics from Abdul Wali Khan University in 2024, followed by his MPhil in Physics during 2024–2026. His MPhil research focused on the growth of Halide perovskite for X-ray imaging. During his undergraduate studies, his research in Materials Science Particularly on perovskite solar cells, and the development of advanced materials for energy conversion and storage applications. (Email: javidamir611@gmail.com)

Atta Ullah earned his BS degree in Physics from Abdul Wali Khan University in 2024. He is currently pursuing his MPhil degree from the same institution. His research interests include Metal–Organic Frameworks (MOFs), Prussian Blue Analogues for energy storage and biomedical applications, and perovskite solar cells, with a focus on advanced functional materials for energy and healthcare technologies. (Email: khanattaullah052@gmail.com)

Adnan Sadiq his BS in Physics from Abdul Wali Khan University in 2024. He subsequently completed his MPhil in Physics during 2024–2026 from the same institution. His undergraduate research focused on Materials Science, particularly the development of advanced materials for energy conversion and storage devices. (Email: sadiqadnan436@gmail.com)

Ibrar Ahmad is currently pursuing his PhD in Medical Physics in Sapienza Università di Roma, Italy and completed his MPhil and BS in Physics from Abdul Wali Khan University Mardan (AWKUM). His research was focused on Materials Science, with particular emphasis on the design, synthesis, and characterization of advanced materials for energy storage devices. Through his research work, he gained valuable experience in materials fabrication, structural and electrochemical characterization techniques, and the evaluation of materials for high-performance energy conversion and storage applications. (Email: ibrar.ahmad@uniroma1.it)

Khizar Hayat is Professor of Physics at Abdul Wali Khan University Mardan, Khyber Pakhtunkhwa, Pakistan. He received his PhD in Physics from Pakistan Institute of Engineering and Applied Sciences in 2014 and completed his postdoctoral research in China in 2018. Throughout his academic career, he has been actively engaged in advanced research in materials science and applied physics. His research interests include condensed matter physics, nanomaterials, nanogenerators, and optoelectronic devices, with a particular focus on developing functional materials for energy harvesting, sensing, and next-generation electronic applications. (Email: khizarhayat@awkum.edu.pk)

Said Karim Shah, Professor of Physics at Abdul Wali Khan University, Pakistan. He earned his PhD in Physics from University of Camerino in 2012 and completed his postdoctoral research at Institut Polytechnique de Bordeaux in 2014. His research interests include TiO_2 and ZnO nanostructures, organic solar cells, organic–inorganic semiconductor devices, nanogenerators, and advanced materials for energy-related applications. (Email: saidkarim@awkum.edu.pk)